J Solid State Electrochem (2009) 13:1715–1722
DOI 10.1007/s10008-008-0728-7

ORIGINAL PAPER

Neural networks for Nyquist plots prediction during corrosion inhibition of a pipeline steel

D. Colorado-Garrido · D. M. Ortega-Toledo · J. A. Hernández · J. G. González-Rodríguez · J. Uruchurtu

Received: 19 August 2008 / Revised: 20 October 2008 / Accepted: 3 November 2008 / Published online: 4 December 2008

Abstract This paper presents a predictive model for electrochemical impedance Nyquist plots using artificial neural network. The proposed model obtains predictions of imaginary impedance based on the real part of the impedance as a function of time. The model takes into account the variations of the real impedance and immersion time of steel in a corrosive environment, considering constant carboxyamido-imidazoline corrosion inhibitor concentrations (5 and 25 ppm). For the network, the Levenberg–Marquardt learning algorithm, the hyperbolic tangent sigmoid transfer function, and the linear transfer function were used. The best-fitting training data set was obtained with five neurons in the hidden layer for 5 ppm of inhibitor and two neurons in the hidden layer for 25 ppm of inhibitor, which made it possible to predict the efficiency with accuracy at least as good as that of the theoretical error, over the whole theoretical range. On the validation data set, simulations and theoretical data test were in good agreement with an R value of 0.984 for 5 ppm and 0.994 for 25 ppm of inhibitor. The developed model can be used for the prediction of the real and imaginary parts of the impedance as a function of time for short simulation times.

D. Colorado-Garrido · D. M. Ortega-Toledo · J. A. Hernández · J. G. González-Rodríguez (✉) · J. Uruchurtu
Centro de Investigación en Ingeniería y Ciencias Aplicadas (CIICAp), Universidad Autónoma del Estado de Morelos (UAEM),
Av. Universidad #1001, Col. Chamilpa,
Cuernavaca, Morelos C.P. 62209, México
e-mail: ggonzalez@uaem.mx

Keywords Neural network · Corrosion inhibitor · Electrochemical impedance

Introduction

Corrosion is one of the main problems in the oil and gas production and transportation industries. Oilfield corrosion manifests itself in several forms, which include the "sweet corrosion" generated by carbon dioxide (CO_2) and/or the "sour corrosion" generated by hydrogen sulfide (H_2S), in water injection systems. The most prevalent form of attack found is produced by the presence of oxygen (O_2) [1]. Inhibitors are currently used to protect against corrosion in all petrochemical facilities in the world because it is cost-effective and flexible. Nitrogen-based organic inhibitors, such as imidazolines or their salts, have been successfully used in these applications even without an understanding of the inhibition mechanism [2].The corrosion inhibition by organic compounds is related to their adsorption properties. Adsorption depends on the nature and the state of the metal surface (microstructure and chemical composition), on the type of corrosive environment, and on the chemical structure of the inhibitor [3]. According to [4], inhibitors incorporate into the corrosion product layer and form a protective barrier between the base metal and the corrosive media. It is suggested that the structure of the inhibitor must be appropriate to interact with the corrosion products and that they can be effective on iron carbonates or sulfides, but not effective on oxides. This work extends the study presented in a previous work [5] with applications of neural networks to electrochemical techniques. This model can be used to predict different impedance Nyquist plots from

different inhibitor concentrations (5 and 25 ppm) without experimental variations in the time domain. Data evaluation was carried out using the technique called electrochemical impedance spectroscopy in an environment containing NaCl and CO_2 to simulate environments found in the transport or crude oil industry. Neural network model was developed and trained with experimental data from electrochemical impedance to know the performance of carboxy-amido-imidazoline as corrosion inhibitor. The obtained results using the neural network model was compared with tested experimental data.

Electrochemical impedance spectroscopy is an electrochemical technique used in corrosion studies. This method uses an alternating current (AC) that is applied over an electrode to obtain the corresponding response. The impedance describes the electric circuit response analogous to an equivalent electrochemical interphase. In an electric circuit of direct current, Ohm's law defines the relation between current (I) and potential (E) as:

$$E = IR. \tag{1}$$

In the case of an alternating signal, the equation is:

$$E = IZ. \tag{2}$$

In Eq. 2, Z represents the total impedance of an electric circuit, in ohms. The AC impedance of an electric circuit depends on the frequency of the applied signal. The complex impedance $Z(j\omega)$ can be represented with the Nyquist plot and it is composed of a real (Z_{re}, X-axis) part and an imaginary part (Z_{im}, Y-axis):

$$Z = Z_{re} + Z_{im} = R_s + R_{ct}/[1 + (j\,\omega C_{dl} R_{ct})] \tag{3}$$

where ω is the depression angle, R_s is the solution resistance, and R_{ct} and C_{dl} are the electrochemical double layer or charge transfer resistance and capacitance, respectively. Notice that, in this plot, the Y-axis is negative and that each point on the Nyquist plot is the impedance at one frequency. Figure 1 has been annotated to show that low-frequency data are on the right side of the plot and higher frequencies are on the left.

From the impedance plot in the Nyquist format, the solution resistance can be obtained from the high-frequency limit of Z_{re} (Z), the addition of the solution and the polarization resistances are equal to the low-frequency limit of Z_{re}, and the capacitance can be calculated from the known frequency at the top of the R_p semicircle, as shown in Fig. 1.

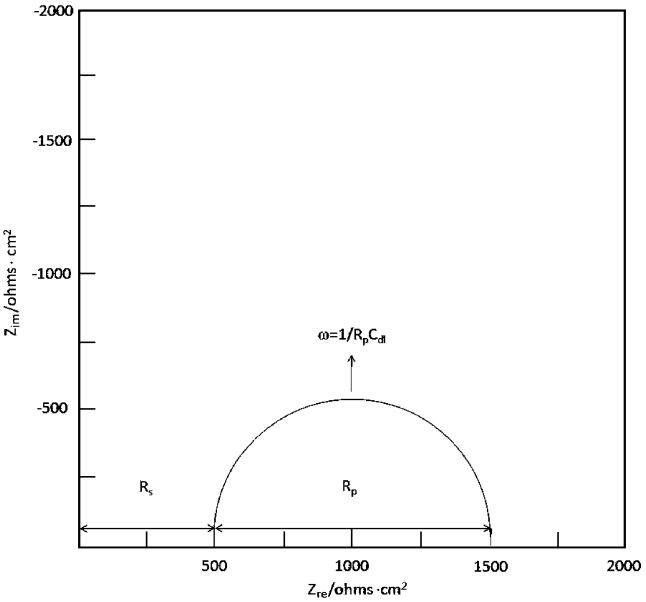

Fig. 1 Typical Nyquist plot

Materials and methods

Neural network systems

The neurons are grouped into distinct layers and interconnected according to a given architecture. As in nature, the network's function is determined largely by the connections between elements (neurons). Each connection between two neurons has a weight coefficient attached to it. The standard network structure for an approximation function is the multiple-layer perception (or feedforward network). The feedforward network often has one or more hidden layers of sigmoid neurons followed by an output layer of linear neurons [6]. Multiple layers of neurons with nonlinear transfer functions allow the network to learn nonlinear and linear relationships between input and output vectors. The linear output layer lets the network produce values outside the −1 to +1 range [7]. For the network, the appropriate notation is used in two-layer networks [8]. A simplified sketch of the network's structure and behavior is presented in Fig. 2 where k is the input variables number, ln is the input variables, Out is the output variables, and the thick lines are weights and biases. The number of neurons in the input and output layers is given, respectively, by the number of input and output variables in the process under investigation.

The optimal number of neurons in the hidden layer(s) n_s is difficult to specify and depends on the type and complexity of the process or experimentation. This number is usually iteratively determined. Each neuron in the hidden

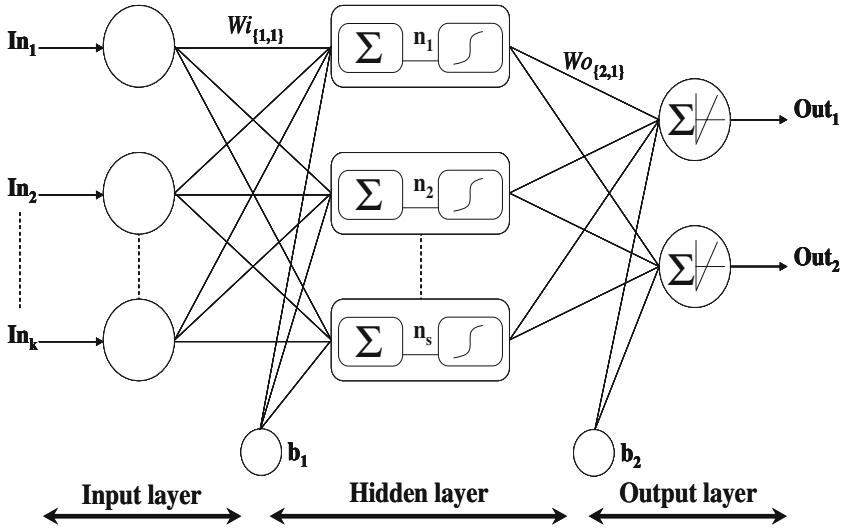

Fig. 2 The neural network computational model

layer has a bias b, which is added to the weighted inputs to form the neuron input n (Eq. 3). This addition, n, is the argument of the transfer function f:

$$n = \mathrm{Wi}_{\{1,s\}}\,\mathrm{In}_1 + \mathrm{Wi}_{\{2,s\}}\,\mathrm{In}_2 + \ldots + \mathrm{Wi}_{\{k,s\}}\,\mathrm{In}_k + b_1. \quad (4)$$

The associated coefficients with the hidden layer are grouped into matrices Wi (weights) and b_1 (biases). The output layer computes the weighted addition of the signals provided by the hidden layer, and the associated coefficients are grouped into matrices Wo and b_2. Using the matrix notation, the network output can be given by Eq. 4:

$$\mathrm{Out} = f[\mathrm{Wo} \times g(\mathrm{Wi} \times \mathrm{In} + b_1) + b_2]. \quad (5)$$

Hidden layer neurons may use any differentiable transfer function to generate their output. In this work, a hyperbolic tangent sigmoid transfer function and a linear transfer function were used for f and g, respectively [8]. From Eq. 4 and considering the transfer functions, the neural network model is Eq. 6:

$$\mathrm{Out} = \sum_s \left\{ \mathrm{Wo}_{(l,s)} \cdot \left[\frac{2}{1 + e^{-2\cdot\left(\sum_k \mathrm{Wi}_{(s,k)}\cdot \mathrm{In}_k + \mathrm{b}_{1(s,l)}\right)}} - 1 \right] \right\} + b_{2(l,1)}. \quad (6)$$

The number of network coefficients (weights and biases) is given by Eq. 7:

$$m = n(\mathrm{In} + 1) + \mathrm{Out}(n + 1). \quad (7)$$

Learning algorithm

A learning (or training) algorithm is defined as a procedure that consists of adjusting the coefficients (weights and biases) of a network to minimize an error function (usually a quadratic one) between the network outputs for a given set of inputs and the correct (already known) outputs. If smooth, nonlinearities are used, the gradient of the error function can be computed by the classical backpropagation procedure [9]. In this work, the Levenberg–Marquardt algorithm optimization procedure in the Matlab Neural Network Toolbox [9] was used. This algorithm is an approximation of Newton's method, which was designed to approach second-order training speed without having to compute the Hessian matrix [10]. The root mean square error (RMSE) is calculated with the theoretical values and network predictions. This calculation is used as a criterion for model adequacy shown in Fig. 3.

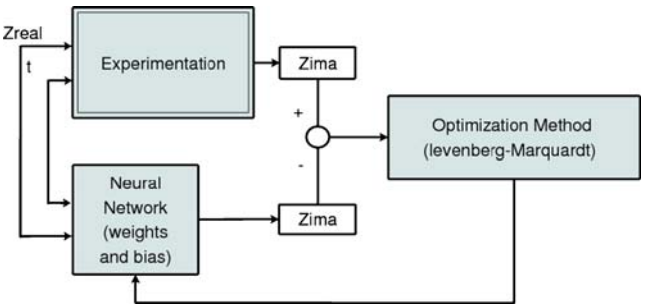

Fig. 3 Recurrent network architecture for the efficiency values and the procedure used for neural network learning

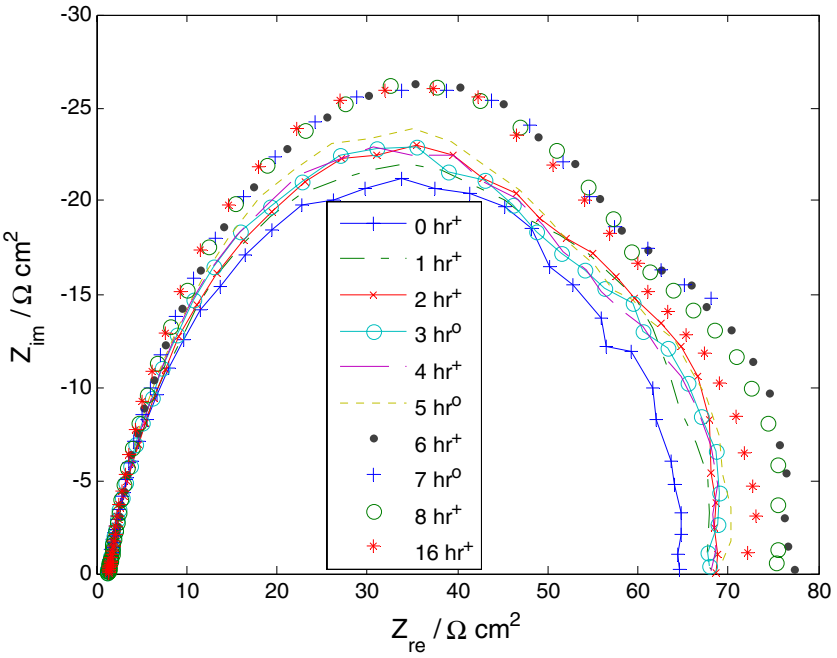

Fig. 4 Experimental conditions studied for 5-ppm inhibitor concentration. *Plus symbols*, learning database; *open circles*, test database

Database preparation

Experimental data provided by Ortega-Toledo [11] were used. The electrochemical techniques used in this study included Nyquist plots. Material tested was a carbon steel–manganese with its main chemical composition as: vanadium 0.001 wt.%, niobium 0.055wt.%, and titanium 0.014 wt.%. Samples of 0.030×0.010×0.30 m were heated at 1,250 °C at a heating rate of 0.4 °C/s, soaked for 90 min, and immediately hot rolled. The rough rolling of the slab was performed from 1,250 to 1,098 °C in five steps, reaching 42.3% of total deformation and an average strain rate of 2.48 s^{-1}. Then, the rough rolling was followed by a cooling period until an experimental initial temperature for the final rolling procedure of 1,051 °C was reached, ending at 867 °C, achieving a total deformation of 37% in five steps with an average strain rate of 2.98 s^{-1}. Immediately after the last final rolling step, the plates were cooled in forced nitrogen gas. This procedure was performed from 867 to 650 °C and then the plates were left to cool in air down to room temperature. Before testing, the electrode was polished using 600 grit SIC emery paper and then cleansed with alcohol, acetone, and distilled water. Inhibitor used in this work was a commercial carboxyamido-imidazoline. The inhibitor was dissolved in

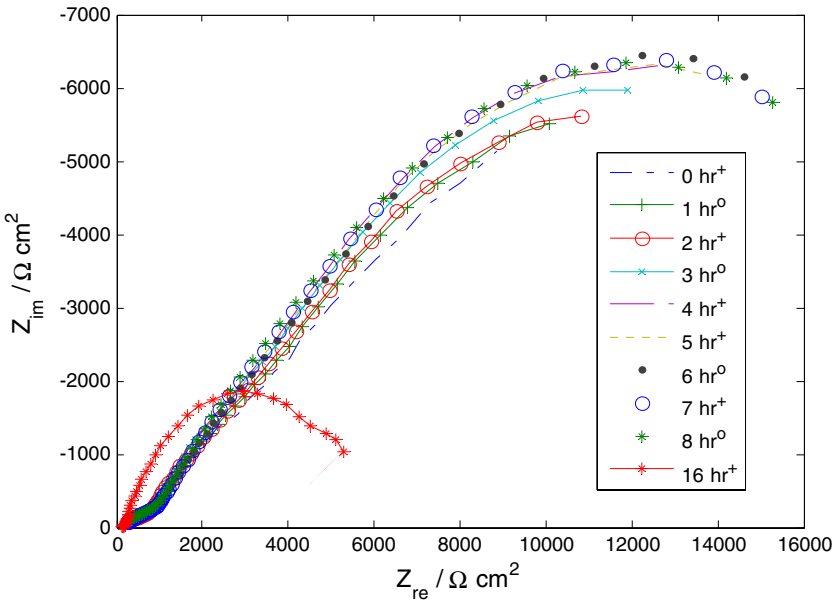

Fig. 5 Experimental conditions studied for 25-ppm inhibitor concentration. *Plus symbols*, learning database; *open circles*, test database

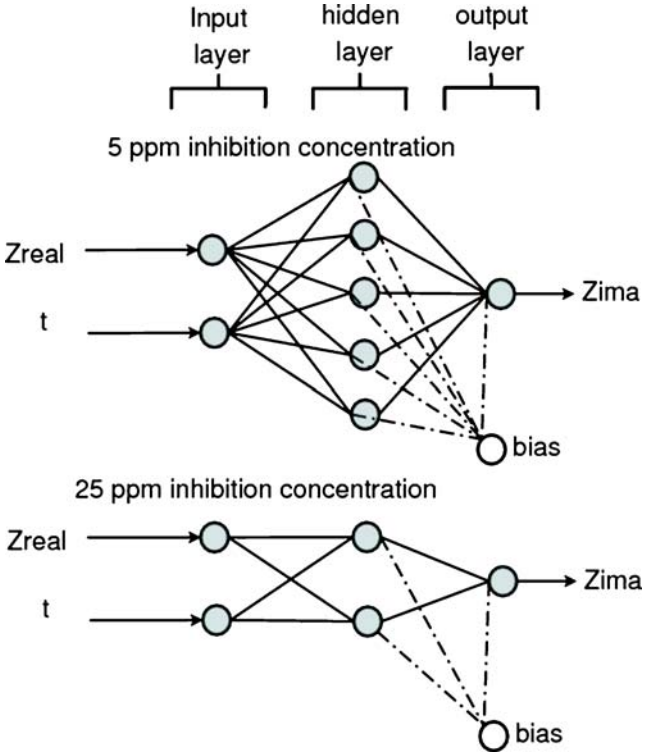

Fig. 6 Neural architecture

pure 2-propanol. The concentrations of the inhibitor used in this work were 5 and 25 ppm and the temperature was kept at 50 °C. Before applying the inhibitor, a solution containing 3% NaCl was prepared. The testing solution consisted of 3% NaCl solution, heated, de-aerated with nitrogen gas, CO_2-saturated for 2 h, and then the inhibitor was added. Continuous stirring and CO_2 bubbling during the tests was used. Electrochemical impedance spectroscopy tests were carried out at the free corrosion potential, E_{corr}, by using a signal with amplitude of 10 mV and a frequency interval of 0.1–100 KHz applied with a model PC4 300 Gamry potentiostat. Tests were carried out during 16 h.

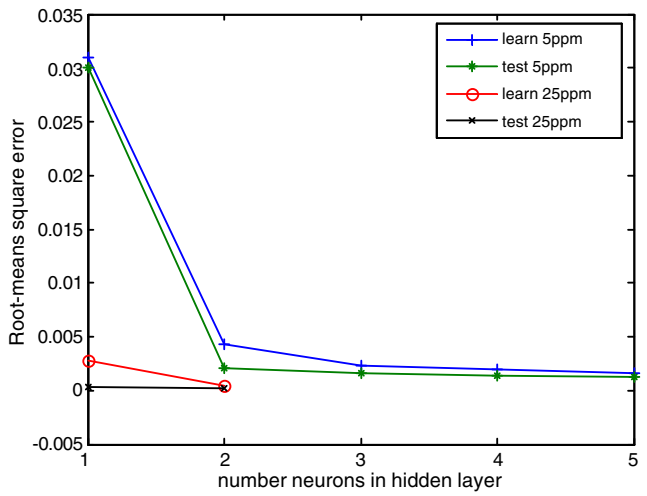

Fig. 7 Comparison of RSME learn and test vs. the number of neurons

Results and discussion

Figures 4 and 5 show the Nyquist plots obtained for the steel in the chloride solution containing 5 and 25 ppm of inhibitor. Thus, the obtained experimental database were split into two parts: learning (75% of database) and testing (25% of database) to build a good representation of the diverse situation. With the Nyquist plot obtained for 5 ppm of inhibitor during 0, 1, 2, 4, 6, 8, and 16 h, immersion data set were used for training the neural network model. In the same way, it was proceeded with the Nyquist plots obtained for 25 ppm of inhibitor used for the learning purpose. Figure 4 shows the experimental conditions; 588 registered data constitute the polarization resistance of the corrosion system with regard to the 5-ppm inhibitor concentration and 650 experimental registered data constitute (Fig. 5) the Nyquist plot for the 25-ppm inhibitor. We can observe that the semicircles have the presence of a second semicircle at low frequencies. Two semicircles indicate the existence of two processes taking place in the system (corrosion process and inhibitor process). During the first 8 h, the polarization or charge transfer resistance (R_{ct}) takes values between 60 and 75 Ω cm^2, increasing its value as time elapses. Figure 5 presents the Nyquist diagram for 25 ppm of inhibitor, and

Table 1 Adjusted parameters for the best neural network

Inhibitor concentration, 5 ppm	
Wi_1	$\begin{pmatrix} -0.0010 & 2.4512 \\ -17.8495 & 0.0224 \\ 17.0354 & 0.2229 \\ -0.0864 & 3.7700 \\ 14.1339 & -14.4833 \end{pmatrix}$
Wo_2	$(-2.7337 \quad 2.2228 \quad 2.2913 \quad 9.8007 \quad 1.7545)$
b_1	$\begin{pmatrix} -3.0916 \\ 7.3080 \\ -7.0004 \\ 1.4536 \\ 13.2605 \end{pmatrix}$
b_2	(-13.2839)
Inhibitor concentration, 25 ppm	
Wi_1	$\begin{pmatrix} -29.1126 & -20.0795 \\ -0.0896 & 2.6110 \end{pmatrix}$
WO_2	$(0.2270 \quad -0.7002)$
b_1	$\begin{pmatrix} 32.6936 \\ 0.5999 \end{pmatrix}$
b_2	(0.1142)

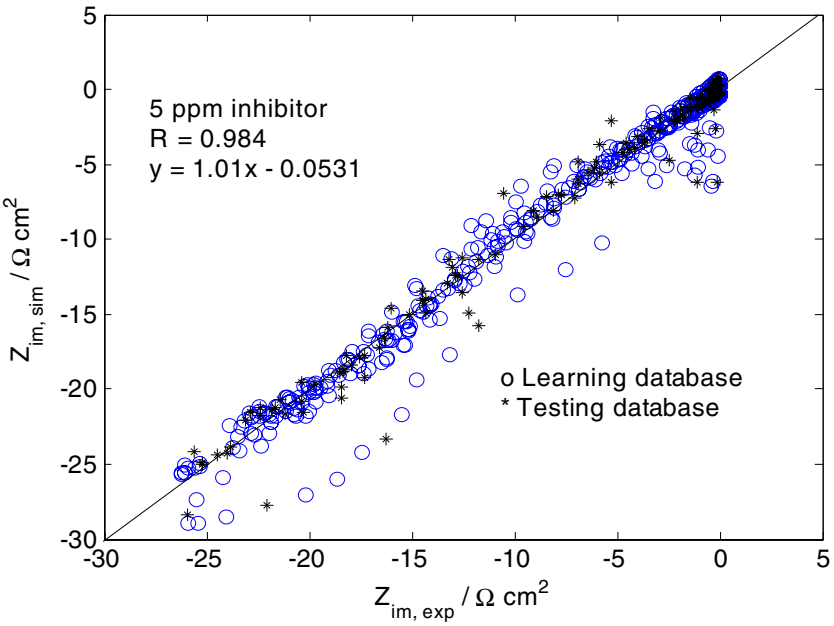

Fig. 8 Comparison of simulated and experimental Z values for 5 ppm of inhibitor

the evolution of the system can be observed showing what is known as Warburg or diffusion-controlled impedance, indicated by a straight line. This slope indicates that the process was controlled by the diffusion of species through the inhibitor-formed layer.

The neural network model which was developed (Fig. 6) involved five and two neurons to determine the imaginary impedance evolution (in ohms square centimeter) for different immersion times obtained for a constant inhibitor concentration. The input layers for these neural network models were real impedance (in ohms square centimeter) and time (in hours).

Learning base for the models

One of the problems that occur during neural network training feedforward is called "overfitting" [8]. To determine the number of neurons of the hidden layer, the RMSE (learning and test database) against the number of neurons was plotted; this comparison is shown in Fig. 7. Therefore, the error in the learning database decreased as the number of neurons increased. The optimal number of neurons in the hidden layer is five for the neural network model of 5 ppm, whereas for the model of 25 ppm of inhibitor was two. Table 1 gives the results for the best fits of the number of

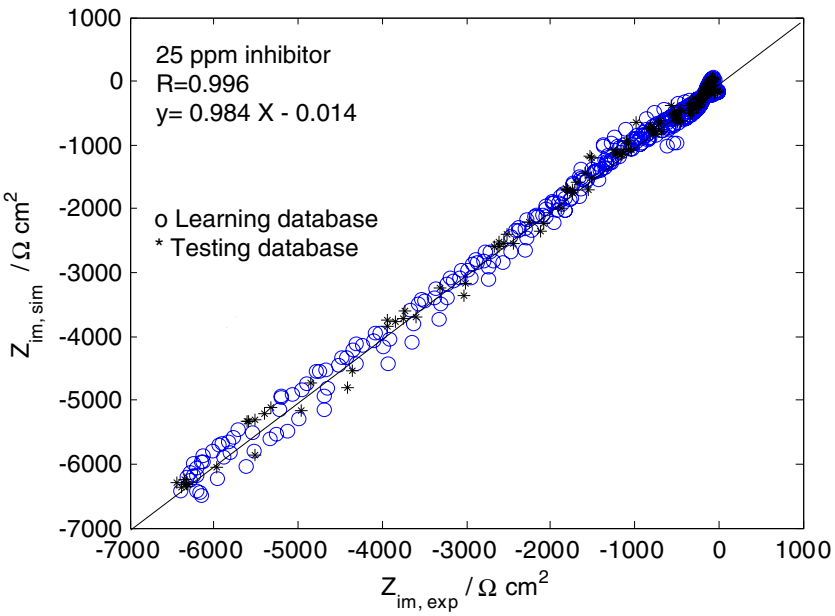

Fig. 9 Comparison of simulated and experimental Z values for 25 ppm of inhibitor

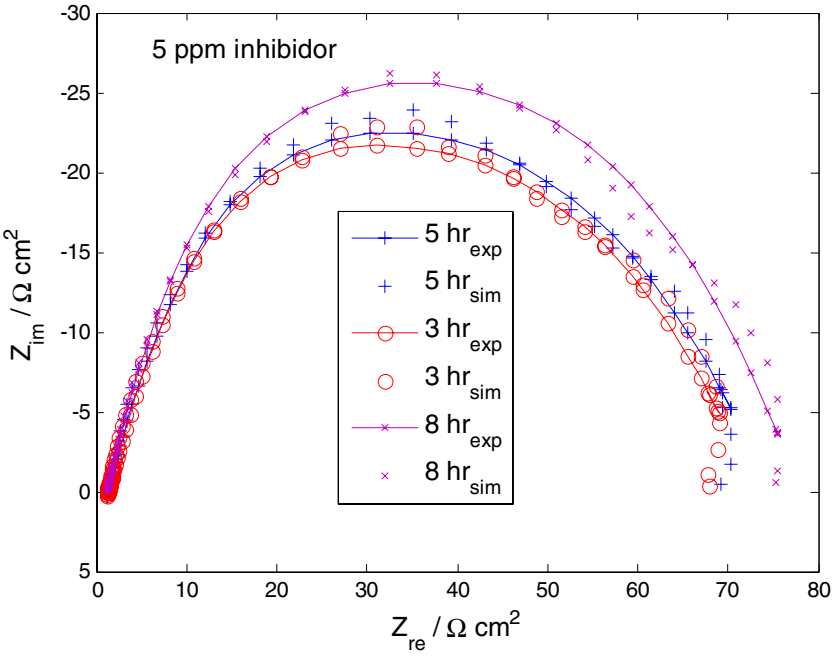

Fig. 10 Comparison of experimental and simulated Nyquist plots for 5 ppm of inhibitor

neurons in the hidden layer, as well as the weight values, biases values for these models.

Validation of the proposed model

Figure 8 presents the simulated imaginary impedance against experimental imaginary impedance database for all Nyquist plots for 5 ppm of inhibitor. This figure shows that the obtained prediction was good and reflected in the regression coefficient of R=0.984. The residuals in the testing database were small and their distribution acceptable and, to confirm this regression coefficient, the test of lack of fit (LOF) was carried out to assure the dispersion inherent in the data. As a result of this test, F^* was 0.08, and according to hypothesis for an α value of 0.01, the F statistic value was 1.3. Consequently, we reject the null hypothesis in favor of the alternative which is lack of the linear fit [12]. The model thus developed was able to predict the imaginary impedance as a function of input parameters throughout the experimental domain.

Figure 9 shows the simulated imaginary impedance against experimental imaginary impedance data for all

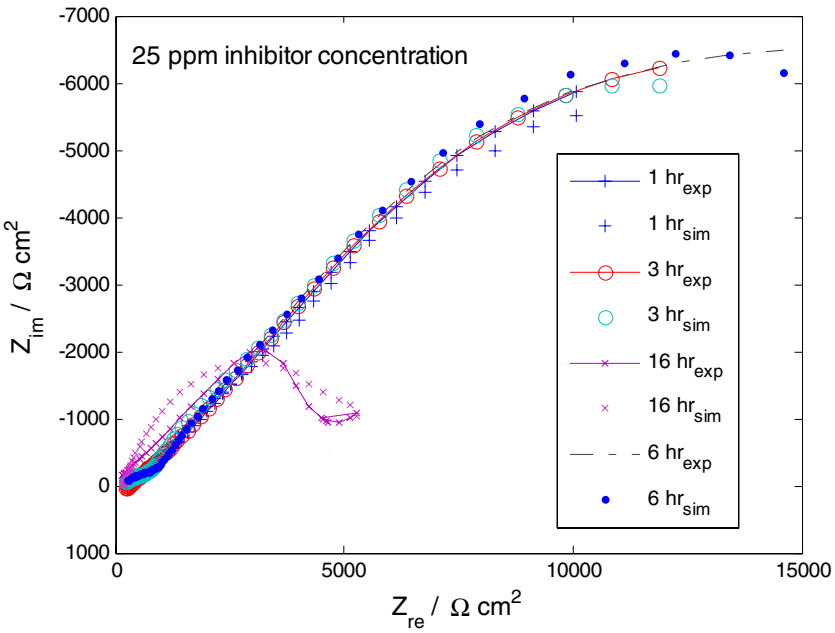

Fig. 11 Comparison of experimental and simulated Nyquist plots for 25 ppm of inhibitor

Nyquist plots for 25 ppm of inhibitor. This figure shows that the prediction was also adequate, reflected in the regression coefficient R=0.996. Similarly, the residuals in the testing database were small and their distribution well balanced, and to confirm this regression coefficient the test of LOF was also carried out to guarantee the dispersion inherent in the data. As a result of this test, F^* is 0.04, and according to hypothesis for an α value of 0.01, the F statistic value was 1.38. Consequently, we also reject the null hypothesis in favor of the alternative which is lack of the linear fit [12]. The model thus developed was also able to predict the imaginary impedance for 25 ppm of inhibitor as a function of input parameters throughout the experimental domain.

Figure 10 depicts the ability of the model to predict the impedance value as a function of time for 5 ppm of inhibitor, whereas Fig. 11 shows the model to predict the impedance as a function of time for 25 ppm of inhibitor. These models are important to determine the corrosion resistance over this experimental condition. It is evident that the models were successful in predicting the impedance value as a function of time. This model is not too complex because the simulation is performed by simple arithmetic operations and, therefore, it can be used to predict Nyquist plots over different immersion times and to determine different impedance behavior with confidence.

Conclusions

This work extends the applications of neural networks in electrochemical impedance techniques. This study shows a neural networks modeling, which can be used for good-quality simulation of imaginary impedance in the Nyquist plots (R=0.984 for 5 ppm of inhibitor and R=0.996 for 25 ppm of inhibitor). These models were validated with experimental electrochemical data, predicting Nyquist plots to determine the corrosion resistance of the tested material in the solution. This model is not complex because the simulation is achieved via simple arithmetic operations, and therefore it can be used for the estimation of the electrochemical impedance over a wide range of experimental conditions. The interest in this kind of modeling must be related to the fact that it is developed without any preliminary assumptions on the underlying corrosion or chemical mechanisms.

References

1. Kermani MB, Morshed A (2003) Corrosion 59:659
2. Xue-Yuan Z, Feng-Ping W, Yu-Fang H, Yuan-Long D (2001) Corros Sci 43:1417. doi:10.1016/S0010-938X(00)00160-8
3. Bentiss F, Lagrenee M, Traisnel M, Hornez JC (1999) Corros Sci 41:789. doi:10.1016/S0010-938X(98)00153-X
4. Rosenfeld IL, Bongomolov DB, Gorodetskii AE, Kazanskii LP, Frolova LV, Shamova LI (1982) Zaschita Metallov 18:163
5. Colorado-Garrido D, Ortega-Toledo DM, Hernández JA, González-Rodríguez JG (2007) Proceedings of the CERMA, Electronics, Robotics and Automotive Mechanics Conference, Cuernavaca, Morelos, Mexico, p 213
6. Vanderplaats GN (1984) Numerical optimization techniques for engineering design. McGraw-Hill, New York
7. Hornik K, Stinchcombe M, White H (1989) Neural Netw 2:359. doi:10.1016/0893-6080(89)90020-8
8. Hernández-Pérez JA, García-Alvarado MA, Trystram G, Heyd B (2004) Innovative Food Science and Emerging Technologies 5:57. doi:10.1016/j.ifset.2003.10.004
9. Natrick MA (1998) in Demuth H, Beale M (eds) Neural network toolbox for Matlab—user's guide. The Math Works, Natick, MA
10. Martin T, Hagan MT, Mohammad BN (1994) IEEE Trans Neural Netw 6:989
11. Ortega-Toledo DM (2007) An electrochemical study of the CO_2 corrosion inhibition of a pipeline steel for crude oil (Estudio electroquímico de la inhibición de la corrosión por CO_2 de un acero para ductos de petróleo crudo). M.Sc. dissertation, Autonomus University of Morelos State, México
12. Neter J, Kunter MH, Nachtsheim CJ, Wsserman W (1996) Applied linear statistical models, 4th edn. McGraw-Hill, USA